Automatika

Journal for Control, Measurement, Electronics, Computing and Communications

ISSN: (Print) (Online) Journal homepage: https://www.tandfonline.com/loi/taut20

Modified Seagull Optimization Algorithm based MPPT for augmented performance of Photovoltaic solar energy systems

Annapoorani Subramanian & Jayaparvathy Raman

To cite this article: Annapoorani Subramanian & Jayaparvathy Raman (2022) Modified Seagull Optimization Algorithm based MPPT for augmented performance of Photovoltaic solar energy systems, Automatika, 63:1, 1-15, DOI: 10.1080/00051144.2021.1997253

To link to this article: https://doi.org/10.1080/00051144.2021.1997253

Published online: 09 Nov 2021.

AUTOMATIKA
2022, VOL. 63, NO. 1, 1–15
https://doi.org/10.1080/00051144.2021.1997253

Modified Seagull Optimization Algorithm based MPPT for augmented performance of Photovoltaic solar energy systems

Annapoorani Subramanian[a] and Jayaparvathy Raman[b]

[a]Department of Electrical and Electronics Engineering, Agni College of Technology, Thalambur, India; [b]Department of Electronics and Communication Engineering, Sri Sivasubramaniya Nadar College of Engineering, Kalavakkam, India

ABSTRACT

The changing weather conditions and Partial Shading Situation (PSS) create numerous challenges in harvesting available maximum power from the solar Photovoltaic (PV) systems. The limitations of classical and bio-inspired optimization-based Maximum Power Point Tracking (MPPT) methods are incapable of extracting maximum power under PSS. Therefore, this paper presents a Modified Seagull Optimization Algorithm (MSOA) based MPPT approach by incorporating Levy Flight Mechanism (LFM) and the formula for heat exchange in Thermal Exchange Optimization (TEO) in the original Seagull Optimization Algorithm (SOA) for accurate tracking of Global Maximum Power Point (GMPP) under transient and steady state operating conditions. The MSOA increases the capability of optimization in finding the optimal value of boost DC-DC converter's duty cycle, D, for operating at GMPP. The superiority of the presented MPPT approach is contrasted with SOA MPPT under uniform irradiation situation and partial shading situations using Matlab Simulink platform. With the presented MSOA MPPT, the settling time and percentage maximum overshoot are reduced by 0.92 times and 0.55 times in comparison to SOA MPPT with increased efficiency. The hardware results validated the simulation results proving the proposed MSOA MPPT as an efficient MPPT for solar PV systems.

ARTICLE HISTORY
Received 10 April 2021
Accepted 11 October 2021

KEYWORDS
Solar Photovoltaic systems; maximum power point tracking; Seagull Optimization Algorithm; partial shading condition; DC-DC boost converter

1. Introduction

Energy from solar Photovoltaic (PV) system is observed as the most efficient sustainable energy compared to energy from fossil fuels since it has the advantages such as low cost, low maintenance, no noise and clean energy. Solar cells convert energy from the Sunlight to DC electrical output using photovoltaic effect [1]. The energy production from PV results in non-steady output power, and its output power is varied according to irradiation, age of panel and temperature [2–5]. PV panels are joined together in different configurations such as series configuration and parallel configuration to form PV array to have higher voltage and current ratings, respectively. PV arrays are normally exposed to uniform irradiation situation and Partial Shading Situation (PSS), and during PSS, the PV array's Power-Voltage (*P-V*) characteristics have many peaks, in which the peak conforming the maximum power is termed as Global Maximum Power Point (GMPP). The other peaks in the *P-V* characteristics of PV array are termed as Local Maximum Power Point (LMPP).

To extract maximum power and to have higher efficiency, the PV array needs to be operated at GMPP by proper setting of DC-DC boost converter's duty cycle. The DC-DC boost converter connects the PV array, and the DC load, and with the help of Maximum Power Point Tracking (MPPT) algorithm, the operation of PV array at GMPP is ensured under dynamic conditions [6]. Various types of MPPT algorithms are proposed in the past. The MPPT methods that are classical include Incremental Conductance (IC), Hill climbing (HC) and Perturb and Observe (P&O) MPPT methods [7,8]. The conventional MPPT methods have advantages such as low cost, ease of implementation and simple, but have drawbacks such as failing to track Maximum Power Point (MPP) during PSS, low speed of convergence and greater oscillations in power.

Soft computing techniques based MPPT methods using Fuzzy Logic Control (FLC) [9], Artificial Neural Network (ANN) [10] and Particle Swarm Optimization (PSO) [11] have the drawbacks such as complexity, high computational time and less speed of convergence. Other bio-inspired soft computing optimization methods namely Bat Algorithm (BA) [12], Ant Colony Optimization (ACO) [13], Artificial Bee Colony (ABC) [14], Cuckoo Search (CS) [15] and Flower Pollination Algorithm (FPA) [16] based MPPT approaches had the ability of tracking GMPP effectively, but suffer from oscillations during the steady-state condition which results in the ineffectiveness of the PV system.

CONTACT Annapoorani Subramanian tannapoorani@gmail.com Department of Electrical and Electronics Engineering, Agni College of Technology, Thalambur, India

Various meta-heuristic optimization methods have been suggested for MPPT such as Whale Optimization Algorithm (WOA) [17], Grey Wolf Optimization (GWO) [18], Salp-Swarm Optimization Algorithm (SSA) [19] and Marine Predator Algorithm [20]. All optimization methods have to address the two phases namely the phase of exploration and phase of exploitation in the search space and need to maintain a right balance among the phase of exploration and the phase of exploitation. The algorithm's exploration phase finds out the various promising areas in the search space while the phase of exploitation exactly finds the optimal solution in the promising field [21,22]. Hence, fine-tuning of both exploration and exploitation phases to be carried out to determine the accurate optimal result in the promising area. The WOA MPPT suffers from easy localization and slow convergence. The GWO algorithm-based MPPT has drawbacks such as sluggish convergence rate, inadequate local searching ability and lesser solving accuracy. The SSA MPPT has limitations such as low precision and low performance during real-time implementation. The Marine Predator Algorithm based MPPT has insufficient exploration capability resulting in getting trapped in local maximums during complex partial shading situations. In spite of huge number of recently proposed optimization methods, the research always focuses on developing more optimization methods according to No Free Lunch (NFL) theorem [23,24]. In accordance to NFL theorem, one optimization method suggested for a specific problem could not guarantee solving all optimization problems due to difference in the nature of the problems. The theorem of NFL motivates researchers in the development of novel optimization techniques for problem-solving in various fields. Seagull Optimization Algorithm (SOA) [25] is one of the latest effective optimization methods, which is gradient-free and applicable to optimize all engineering problems occurring in real life. The improved method of SOA for optimal identification of parameter of PEMFC stacks is discussed in [26]. The proposed algorithm utilizes the Levy Flight Mechanism (LFM) to attain faster rates of convergence. The cost minimization of the grid-connected power generation with hybrid renewable energy system through optimal sizing with modified Seagull Optimization method is proposed in [27]. The exploration capability of SOA is enhanced using LFM to provide accurate solution with less convergence time and the same has not been applied to MPPT application so far. The idea of heat exchange in Thermal Exchange Optimization (TEO) is utilized in SOA to improve the exploitation capability of SOA for feature selection application in [28]. Therefore, this paper suggests a Modified Seagull Optimization Algorithm (MSOA) based MPPT approach for solar photovoltaic systems with uniform irradiation conditions and partial shading situations. The MSOA is developed with the incorporation of LFM and formula for heat exchange in TEO in the original SOA for the purpose of omitting local maxima during PSS with faster convergence rate and accurate determining of GMPP respectively due to the augmented exploration and exploitation capability. The contribution of the paper is mentioned below.

1. Exploration and exploitation capability augmentation of original SOA and determining GMPP
2. Determining GMPP accurately under transient and steady state operating conditions.
3. Decreasing time for convergence.

The paper's remaining content is structured as follows. The PV array's characteristics and the boost DC-DC converter's design are described in Section 2. Section 3 describes the SOA MPPT method and Section 4 discusses the proposed MSOA based MPPT method. The results of simulation are presented in Section 5. The hardware results are presented in Section 6. The conclusion of the paper is discussed in Section 7.

2. Characteristics of PV array and boost DC-DC converter's design

The single diode model of solar panel is chosen for its structural simplicity and result accuracy and is shown in Figure 1. The expression governing this model is represented as,

$$I = N_{SH}\left(I_L - I_0\left[\exp\left(\frac{q(V+IR_s)}{N_S AkT}\right) - 1\right] - \frac{(V+IR_s)}{N_S R_{sh}}\right) \quad (1)$$

where V and I represent the output voltage and output current of solar array respectively, q denotes the electronic charge, N_{SH} and N_S denotes the number of parallel and series-connected solar cells, respectively, I_o indicates the saturation current, I_L indicates the current due to sunlight, A and k represents the ideality factor of the diode and Boltzmann's constant respectively, T denotes the PV cells' temperature measured in Kelvin, and R_{sh} and R_s represents the parallel resistance and series resistance respectively. The solar panel considered for this work is BPMSX 60 and its specifications are listed in Table 1. Figure 2 displays PV array's *P-V*, *I-V* curves under uniform irradiation condition, and the V_{mp} and I_{mp} are the voltage and current agreeing to MPP (P_{max}). The boost DC-DC converter's duty cycle variation is carried out in agreement to the variations in insolation to reap the possible maximum power from the solar array at any time. Figure 3 represents PV array's P-*V*, *I-V* curves under partial shaded situations.

Under PSS, the *P-V*, *I-V* curves have many peaks challenging an outstanding optimization method for determining the optimum boost converter's duty cycle

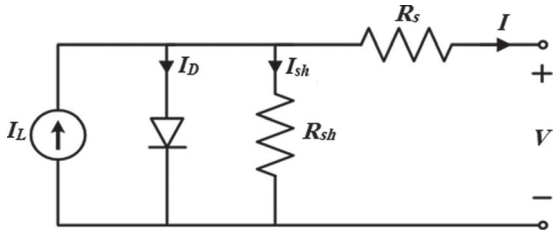

Figure 1. Solar cell's circuit model.

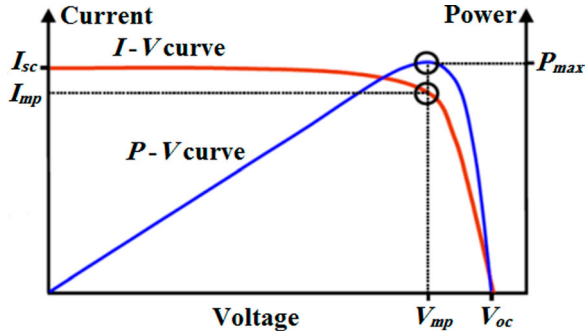

Figure 2. PV array's characteristics under uniform irradiation condition.

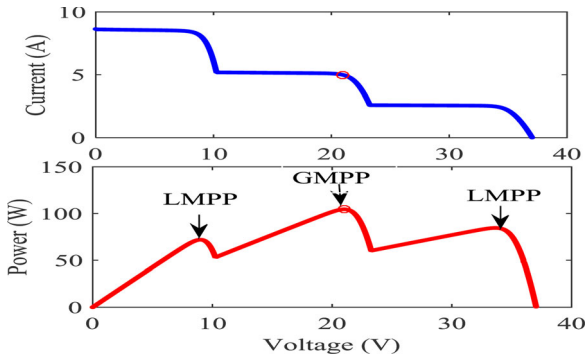

Figure 3. PV array's characteristics under partial shaded situations.

Table 1. Solar panel – BPMSX 60 specifications.

Variables	Value
Voltage during Maximum power, V_{mp} (V)	17.1
Current during Maximum power, I_{mp} (A)	3.5
Maximum power, P_{mp} (W)	60
Open circuit voltage, V_{oc}(V)	21.1
Short circuit current, I_{sc} (A)	3.8

corresponding to GMPP. Figure 4 displays the DC-DC boost converter using MSOA MPPT controller for PV applications. The boost converter joints the DC load and the PV system's solar array, and it is responsible for the change of DC output voltage, which is greater or lesser than the PV array's voltage. For the operation of PV system at maximum efficiency, the boost DC-DC converter's design acts as a major role. The circuit of boost converter contains the power semiconductor switch (MOSFET), *S*, output capacitor, C_{out}, diode, *D*, inductor, *L* and input capacitor, C_{in}. MOSFET

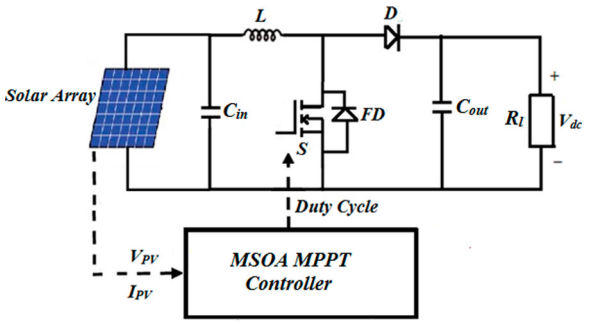

Figure 4. Boost DC-DC converter with MSOA MPPT controller.

Table 2. Boost DC-DC converter's design values.

Parameter	Value
Inductor, *L*	2 mH
Input Capacitor, C_{in}	480 μF
Output Capacitor, C_{out}	0.6 mF
Switching frequency, *fs*	20 kHz
Load resistor, R_l	120 Ohms

switch is frequently adopted for applications operating at low power. The boost converter's input is fed from the PV array, and the PV array's output changes in accordance to the atmospheric condition. In accordance to the changes in the boost DC-DC converter's input from the solar array, the duty cycle of DC-DC boost converter is changed to reap the maximum possible PV system's power. The boost DC-DC converter's design values are computed with the traditional analysis of boost converter and are presented in Table 2. The presented MPPT method is proficient of working with any type of boost DC-DC converters with single switch.

3. Seagull Optimization Algorithm (SOA) based MPPT approach

Seagulls are very intelligent birds that live in the sea in the entire world. They normally eat earthworms, fish, insects; reptiles, etc. and belong to the omnivorous family. Seagulls tend to survive in colonies. The intelligence of seagulls is employed in finding and attacking the prey. The most utilizing behaviours of seagulls are their migration behaviour and behaviour of attacking. The migration, which is a seasonal activity, during which, the seagulls travel from one area to another area in search of the most plentiful and the richest food that is capable of providing sufficient energy. The migration behaviour is explained as below.

- For the duration of migration, seagulls move in group. The initial position of all seagulls will be distinct in the aim of avoiding collisions among themselves.
- In the seagulls group, the other seagulls move towards the seagull that is the fittest and the best in survival.

- The initial positions of other seagulls are updated on the basis of seagull that is the fittest and best in survival.

During migration of seagulls, they attack other birds above the sea which are also in migration. The natural movement of seagulls at the time of attacking will be in the shape of spiral. The migration and attacking behaviour of seagulls could be incorporated for the optimization of the objective function.

3.1. Exploration using behaviour of migration

During the process of migration, the movement of seagulls group from one place to another place is utilized for the phase of exploration. In the exploration phase, the following conditions to be satisfied.

Condition 1: The collision among the other seagulls to be avoided, for which an extra variable X is used in the computation of position of the new searching seagull.

$$\overrightarrow{Z}_s = X * \overrightarrow{U}_s(i) \tag{2}$$

In expression (2), $\overrightarrow{Z}_s$ denotes the search agent's position that does not collide with neighbouring search agents, and $\overrightarrow{U}_s$ denotes the search agent's current position. Current iteration is denoted by i, and the search agent's behavioural movement in the space of search is indicated by X.

$$X = fc - (i * (fc/t)) \tag{3}$$

where, $i = 0, 1, 2 \ldots t$. In expression (3), the variable X's frequency is controlled by f_c and could be linearly reduced from value of f_c to the value of 0. The f_c value is set as 1 in this paper.

$$\overrightarrow{P}_s = Y * (\overrightarrow{Z}_{fs}(i) - \overrightarrow{Z}_s(i)) \tag{4}$$

In expression (4), $\overrightarrow{Ps}$ denotes the $\overrightarrow{Zs}$ search agent's position towards the fittest search agent, $\overrightarrow{Zfs}$ (i.e. fittest seagull). The randomized behaviour of Y is accountable for the correct balance among the exploration phase and exploitation phase. The value of Y is computed using the expression given below.

$$Y = 2 * X^2 * nd \tag{5}$$

In expression (5), n_d is any random number in the range from 0 to 1.

Condition 2: All search agents update its position in accordance to the fittest search agent's position that is fittest seagull's position, so that all search agents remain in close proximity with respect to the fittest search agent.

$$\overrightarrow{D}_s = |\overrightarrow{Z}_s + \overrightarrow{N}_s| \tag{6}$$

In expression (6), $\overrightarrow{D}_s$ denotes the distance amid the fittest search agent and the other search agent.

3.2. Exploitation using behaviour of attacking

The seagulls search processes' experience and history are utilized for the exploitation phase. The speed and the attack angle are changed by the seagulls during migration with retaining of altitude with the help of weight and wings. The movement behaviour of seagulls in the spiral shape helps in prey attacking, and the behaviour in a, b and c planes is mentioned as below.

$$a' = v * \cos(w) \tag{7}$$

$$b' = v * \sin(w) \tag{8}$$

$$c' = v * w \tag{9}$$

$$v = r * e^{kw} \tag{10}$$

Here, v denotes the radius of spiral's each turn; w is any random number in a range of 0–2, e denotes the natural logarithm's base, and r and k are constants that describe the spiral shape.

The search agent's updated position is calculated using the equation given below.

$$\overrightarrow{Z}_s(i) = (\overrightarrow{Ds} * a' * b' * c') + \overrightarrow{Z}_{fs}(i) \tag{11}$$

In expression (11), the best solution is given by $\overrightarrow{Z}_s(i)$ and also it updates other search agents' position. For MPPT, search agent seagulls are considered as duty cycles, and the best seagull is called the best duty cycle and its position represents the best duty cycle value corresponding to GMPP. The population is randomly generated in the SOA. The positions of search agents are updated in accordance to the fittest search agent in each iteration process. X is reduced linearly from the value of f_c to the value of 0. Variable Y is responsible for the smooth transition from exploration phase to exploitation phase.

4. Modified Seagull Optimization Algorithm (MSOA) based MPPT approach

The MSOA MPPT incorporates LFM and formula of heat exchange in TEO to increase the exploration and exploitation capability respectively of original SOA to result in better performance of solar PV system. During PSS, the *P-V*, *I-V* curves have many maximums, and the proposed optimization algorithm for MPPT need to possess high exploration capability to avoid getting trapped at local maximum that results in lower efficiency of solar PV system. The exploration capability of SOA MPPT method can be augmented using the strategy of Levy-Flight (LF) that updates the searching element's position to determine the GMPP during PSS and to reduce the convergence time.

Paul Levy is a mathematician from France who developed Levy-Flight initially. Both artificial and natural phenomena will be having diverse range that is defined in connection with Levy statistics [29]. The

length of steps has values which are dispersed in accordance to stable Levy distribution, which is a random process. The distribution according to Levy is given by the below expression.

$$Levy(\alpha) \sim u = t^{-1-\alpha}, 0 < \alpha \leq 2 \tag{12}$$

In Equation (12), Levy index is denoted by α, which is vital for stability fine-tuning. The random number in Levy is evaluated using the below expression:

$$Levy(\alpha) \sim \frac{\varphi * \mu}{|g|^{1/\alpha}} \tag{13}$$

In Equation (13), both g and μ denote normal standard distributions. Gamma standard function is denoted by Γ, $\alpha = 1.5$, and the below expression defines the term ϕ:

$$\varphi = \left[\frac{\Gamma(1+\alpha) * \sin(\Pi * \alpha/2)}{\Gamma((\frac{1+\alpha}{2}) * \alpha * 2^{\frac{\alpha-1}{2}})} \right]^{1/\alpha} \tag{14}$$

The compromise of exploration capability and exploitation capability of bio-inspired optimization methods can be improved using the strategy formulated by LF strategy that updates the searching element's position given by the expression mentioned below as

$$X_j^{levy} = Xj + Xj \times levy(\alpha) \tag{15}$$

In Equation (15), X_j^{levy} denotes position which is new of j^{th} searching agent after updating X_j. In the exploration phase, the Levy flight involves process, which is random in nature, and the jump size will be following the Levy probability distribution function and prevents the operating point getting trapped in the local maximums during PSS. Hence, the optimal solution given by LFM has higher probability of avoiding local maximums and helps in obtaining GMPP faster.

On the basis of the abovementioned LFM strategy, the solution update equation of MSOA is now calculated using the equation given below.

$$\overrightarrow{D}_s l = \overrightarrow{D}_s + |\overrightarrow{Z}_s + \overrightarrow{P}_s| levy(\alpha) \tag{16}$$

The fitness value for duty cycles, D_{sl} and D_s are calculated. If fitness value P_{PV} of D_{sl} is more than the fitness value P_{PV} of D_s, then $D_{sl} = D_{sl}$, otherwise, $D_{sl} = D_s$.

The updated searching agent's position in MSOA adopting LFM is computed employing the equation given below.

$$\overrightarrow{Z}_s(i) = (\overrightarrow{D}_s l * a' * b' * c') + \overrightarrow{Zf}_s(i) \tag{17}$$

For MSOA MPPT, $\overrightarrow{Z}_s(i)$ denotes the value of duty cycle corresponding to GMPP.

The thermal exchange idea in Thermal Exchange Optimization (TEO) is utilized in SOA to improve the exploitation capability of SOA. TEO is on the basis of Newton's law of cooling, which states that an object's heat loss rate is directly proportional to the temperature differences between the surrounding and the object. According to the algorithm of TEO, some agents are considered as cooling objects and the other agents are considered as the environment. The TEO has outperformed in uni-modal problems in the literature which proves its excellent exploitation performance. Also, TEO proved to have good robustness by having standard deviations that are nearer to zero or equal to zero. The formula for temperature between the objects that are updated is given by the expression given below.

$$T_i^e = (1 - (K_1 + K_2 \times (1-t)) \times random) \times T_i'^e \tag{18}$$

$$t = \frac{p}{P} \tag{19}$$

In expression (18), K_1, K_2 represents control variables, $T_i{}^{e}$ represents object's previous temperature, and $T_i{}^{e}$ represents the updated temperature. In expression (19), P represents the maximum number of iterations and p represents the number of the current iteration. In TEO MPPT, the objects are considered as duty cycles and their positions are considered as duty cycle values and the objective function is maximization of power from PV array to the load.

The updated temperature (duty cycle value) of every object is given by the following expression.

$$T_i^n = T_i^e + (T_i^o - T_i^e) \exp(-\delta t) \tag{20}$$

$$\delta = \frac{\text{PV power of (worst object)}}{\text{PV power of (object)}} \tag{21}$$

In expression (20), T_i^n and T_i^o are the new and old temperature values of the object. If the value of δ is low, the modification of duty cycle takes place slowly in order to get close to the target duty cycle value corresponding to GMPP. Hence, the parameter δ is incorporated in the duty cycle updating equation of SOA for increasing the exploitation capability of the original SOA. The value of δ is calculated using the expression (21).

The Equation (4) in SOA is modified upon incorporation of TEO in SOA to improve the exploitation capability and can now be written as:

$$\overrightarrow{P}_s = Y * (\overrightarrow{Z}_{fs}(i) - \overrightarrow{Z}_s(i)) \times \exp(-\delta t) \tag{22}$$

The algorithm of MSOA MPPT is given below.

Pseudo code Algorithm of MSOA MPPT

Step 1: **Begin**

Step 2: Generate duty cycle's population and initialize X, Y, maximum iterations, t

Step 3: Set the values of f_c to 1, r to 1, w to 1 and i to 1

Step 4: **While** (optimal duty cycle not found or $i < t$) **do**

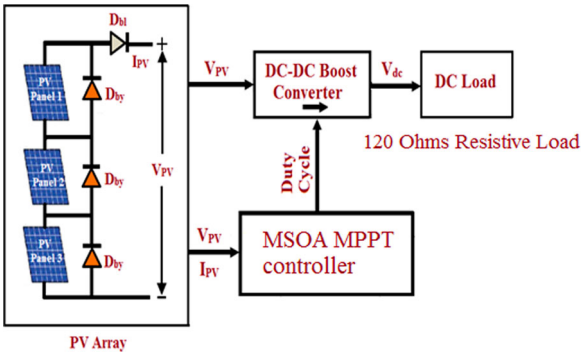

Figure 5. PV system's block diagram using MPPT approach based on MSOA.

Step 5: Computation of fitness function value, $\boldsymbol{P_{PV}}$, for every duty cycle (search agent)

Step 6: Using migration behaviour, n_d value is generated randomly in the range of 0–1

Step 7: Using migration behaviour, w value is randomly produced in the $0–2\pi$ range

Step 8: Using attacking behaviour, generate the value of v

Step 9: Compute, $\overrightarrow{D}_s l$, the distance amid the fittest duty cycle and the other duty cycle using equations (22) and (16)

Step 10: Compute updated value of duty cycle incorporating LFM using equation (17)

Step 11: $i = i + 1$

Step 12: **end while**

Step 13: Return the best duty cycle value corresponding to GMPP

Step 14: **End**

The PV system's block diagram using MPPT approach based on MSOA is displayed in Figure 5. The MSOA MPPT controller receives PV array voltage, V_{PV} and PV array current, I_{PV}, as inputs. In MSOA MPPT controller, the population of duty cycle is generated randomly as 0.1, 0.25, 0.5, 0.75 and 0.85 with a population size of five searching agents. The maximum iterations, t, value is set as 15. The values of f_c, r and w are set as 1. The values of X, Y are computed. When optimal duty cycle value is not found or the iteration number is less than the maximum iterations number, t, the fitness value, P_{PV}, is computed for every duty cycle, and n_d and w values are randomly generated using migration behavior of the search agent, seagull. The value of v is computed using attacking behaviour of the search agent, seagull. Finally, the $\overrightarrow{D}_s l$ value is computed, and the updated value of duty cycle incorporating LFM and TEO is computed using equation (17). The iteration number is incremented and the same steps are repeated till optimal duty cycle is found or the maximum iterations number specified is reached. Finally, the duty cycle's optimal value that corresponds to GMPP is fixed to the boost converter with the employed controller with MSOA approach if expression (23) is not satisfied.

Table 3. Five different irradiation conditions considered for testing the system.

Condition	Solar Panel 1	Solar Panel 2	Solar Panel 3
Uniform Irradiation Condition 1 (UIC1)	1000 W/m^2	1000 W/m^2	1000 W/m^2
Partially Shaded Situation 1 (PSS-1)	1000 W/m^2	800 W/m^2	600 W/m^2
Partially Shaded Situation 2 (PSS-2)	900 W/m^2	800 W/m^2	400 W/m^2
Partially Shaded Situation 3 (PSS-3)	700 W/m^2	600 W/m^2	500 W/m^2
Partially Shaded Situation 4 (PSS-4)	700 W/m^2	500 W/m^2	300 W/m^2

The SOA and MSOA based GMPPT techniques are re-initialized whenever the operating condition changes. The weather conditions' change or partial shaded situations' change are sensed when the relative power change crosses the threshold value of power as given by the expression (23). $P_{PVthreshold}$ value is taken as 0.1. If expression (23) is satisfied, the steps will be carried out from step 2 again in the pseudo code algorithm until the optimal duty cycle corresponding to new GMPP is tracked.

$$\frac{|P_{PVnew} - P_{PVlast}|}{P_{PVlast}} \geq P_{PVthreshold} \tag{23}$$

Then, the optimal value of duty cycle corresponding to GMPP is set to boost DC-DC converter by the MSOA MPPT controller. The flowchart of MSOA MPPT is shown in Figure 6. The proposed MPPT based MSOA is tested with three PV modules which can produce a maximum of three maximums in the P-V curve under PSS. But, owing to the random walk introduced by LFM in the modification of search agent's position and incorporation of heat exchange formula in $\overrightarrow{Ps}$ expression, the MSOA MPPT can perform well for complex partial shading conditions up to even 12 peaks in the P-V Curve with an increase in the number of iterations considered with the increase in complexity.

5. Simulation results

The proposed MSOA MPPT approach is validated under five different irradiation conditions using MATLAB Simulink platform in a solar PV system with PV array of three series-connected solar panels with parallel-connected bypass diodes, D_{by}, across each panel, and a blocking diode, D_{bl}, which is series connected with the solar array, joined to a boost DC-DC converter, which in turn connected to a DC load resistance of 120 ohms. The sampling time of boost converter is taken as 0.05 s. The five different irradiation conditions considered for testing the system are shown in Figure 7 and tabulated in Table 3.

5.1. *Uniform Irradiation Condition 1 (UIC1)*

During this situation, solar panel 1, solar panel 2 and solar panel 3 gets Sun's insolation of 1000 W/m2. The

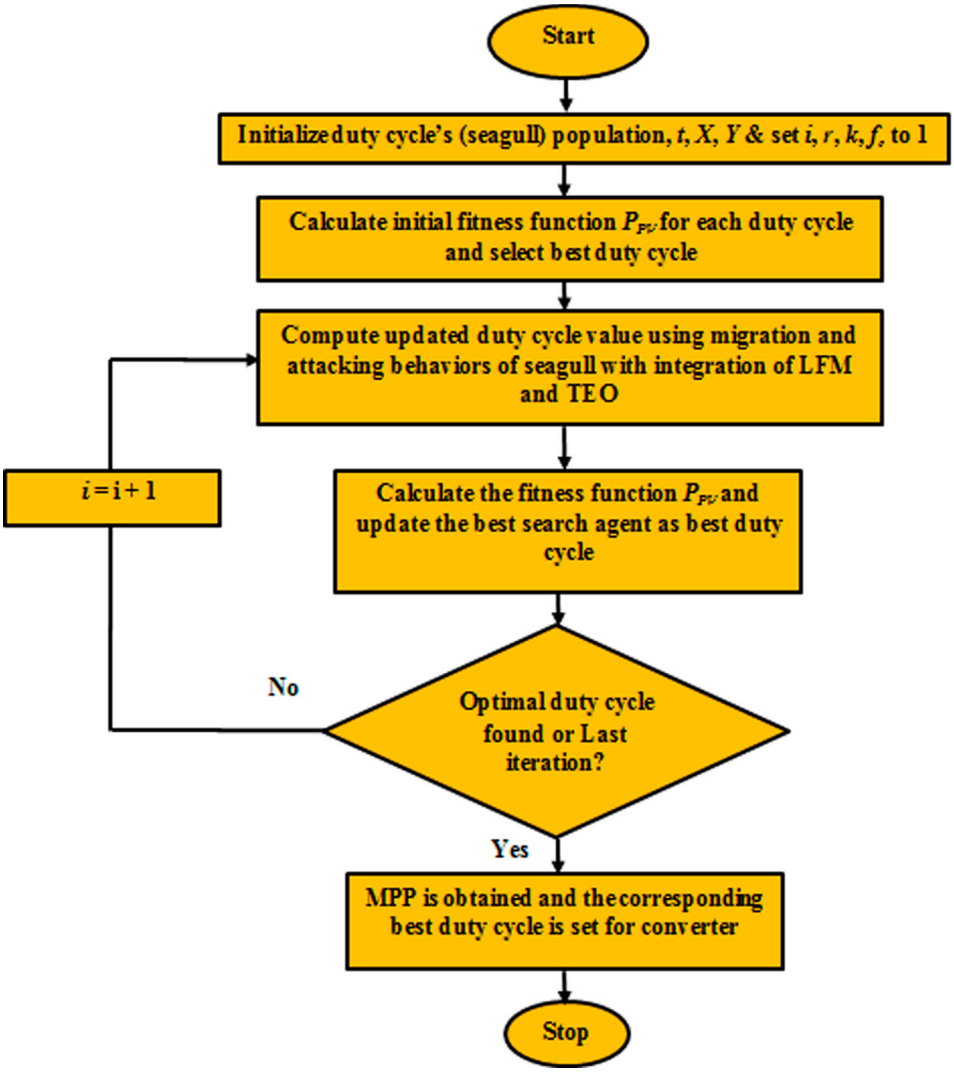

Figure 6. Flowchart of MSOA MPPT.

solar array's Current-Voltage and Power-Voltage characteristic during UIC1 is presented in Figure 8. The comparison curves of voltage of PV array, current of PV array and power of PV array for SOA and MSOA MPPT approaches during UIC1 are shown in Figures 10–12. The duty cycle curve for MSOA and SOA MPPT approaches is shown in Figure 13. Upon observation from Figure 12, the values of PV power for SOA and MSOA MPPT approaches are 178.949 and 179.224 W, respectively. The settling times for SOA and MSOA MPPT approaches are 20.5 and 19 ms, respectively. The response curve's maximum peak value measured with respect to expected system's response is termed as maximum overshoot. Maximum overshoot normally expressed in percentage of the steady-state value termed as percentage maximum overshoot. The MSOA and SOA MPPT approaches' percentage maximum overshoots are 1.62% and 2.95% respectively. The randomness nature introduced by LFM, and the jump size determined by Levy probability distribution function enhanced the exploration capability and convergence speed of SOA that helped in reducing the percentage maximum overshoot and settling time. With the results of simulation, it is clearly observed that maximum power is extracted by the suggested MSOA MPPT approach with less time for convergence and less maximum percentage overshoot during UIC1. The comparison of SOA and MSOA MPPT approaches during UIC1 is displayed in Table 4.

Table 4. Comparison of SOA and MSOA MPPT approaches under UIC1.

Parameter	SOA	MSOA	Actual values
PV Power (W)	178.949	179.224	180
PV current (A)	3.491	3.495	3.5
PV voltage (V)	51.26	51.28	51.3
Duty cycle (%)	61.65	61.68	61.77
Efficiency (%)	99.41	99.56	100
Settling period (ms)	20.5	19	–
Percentage maximum overshoot (%)	2.95	1.62	–

5.2. Partial Shading Situation 1 (PSS-1)

During this situation, solar panel 1, solar panel 2 and solar panel 3 gets Sun's insolation of 1000, 800 and 600 W/m2, respectively. The solar array's Current-Voltage and Power-Voltage characteristic during PSS-1

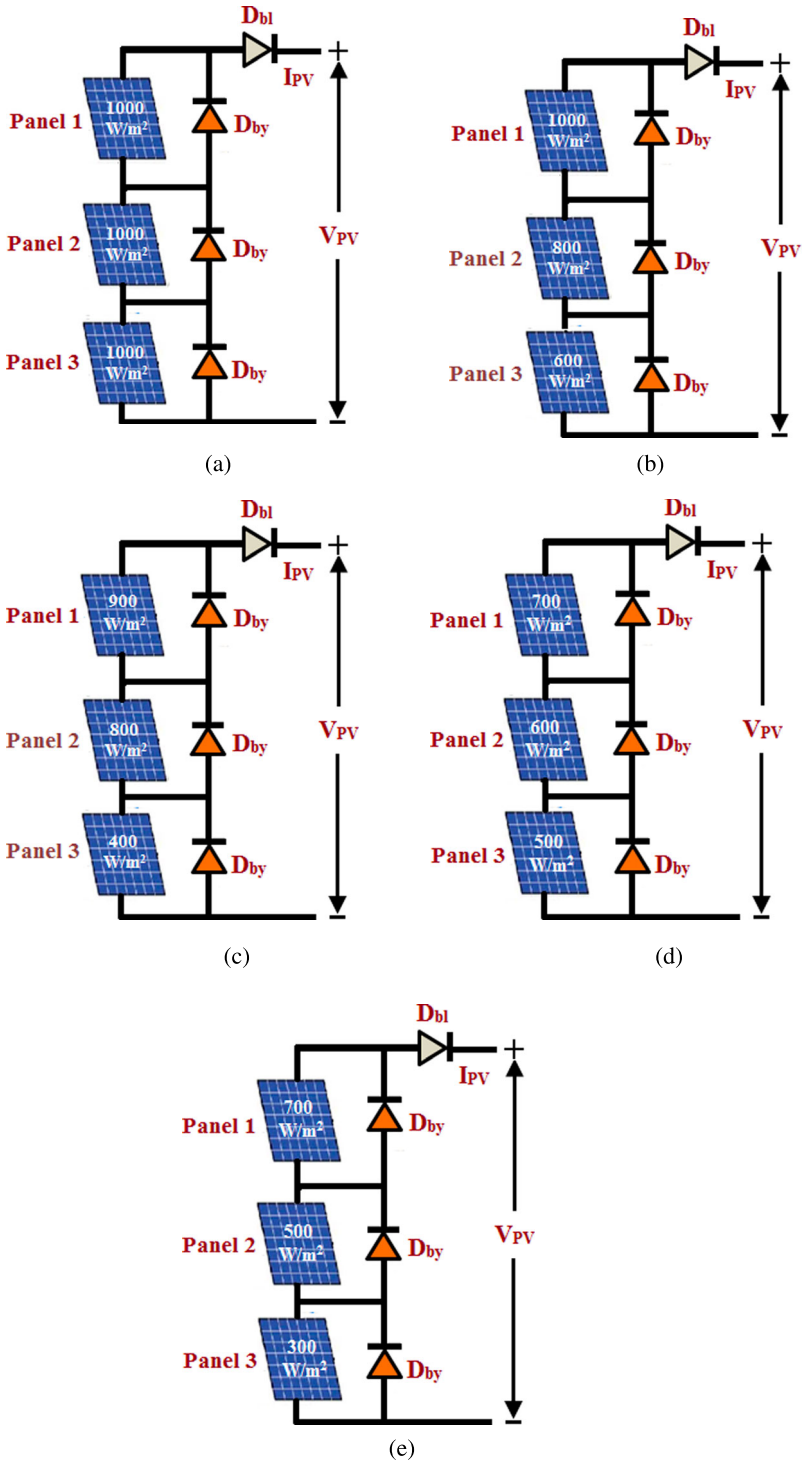

Figure 7. Five different irradiation conditions (a) Uniform Irradiation Condition 1 (b) Partial Shading Situation 1 (c) Partial Shading Situation 2 (d) Partial Shading Situation 3 (e) Partial Shading Situation 4.

is shown in Figure 9. The comparison curves of voltage of PV array, current of PV array and power of PV array for SOA and MSOA MPPT approaches under PSS-1 at 0.2 s are presented in Figures 10–12. The duty cycle curve for MSOA and SOA MPPT approaches is shown in Figure 13 at 0.2 s. Upon observation from Figure 12, the values of PV power are 117.972 and 117.755 W for MSOA and SOA MPPT approaches, respectively, during PSS-1. The settling times for MSOA and SOA MPPT approaches are 20.5 and 21.5 ms, respectively. The MSOA and SOA MPPT approaches' percentage maximum overshoots are 3.02% and 3.92%, respectively. With the results of simulation, it is clearly observed that maximum power is extracted by the suggested MSOA MPPT approach with less time for convergence and less maximum percentage overshoot during PSS-1. The comparison of SOA and MSOA MPPT approaches during PSS-1 is displayed in Table 5.

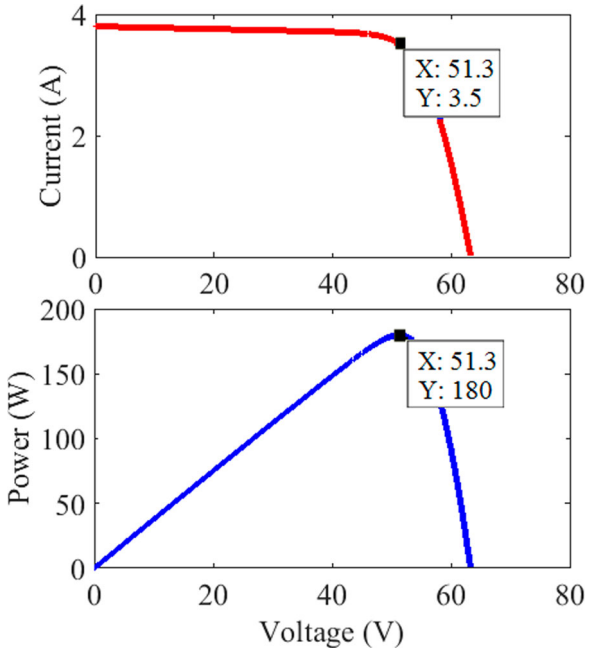

Figure 8. Current-Voltage and Power-Voltage characteristics during UIC1.

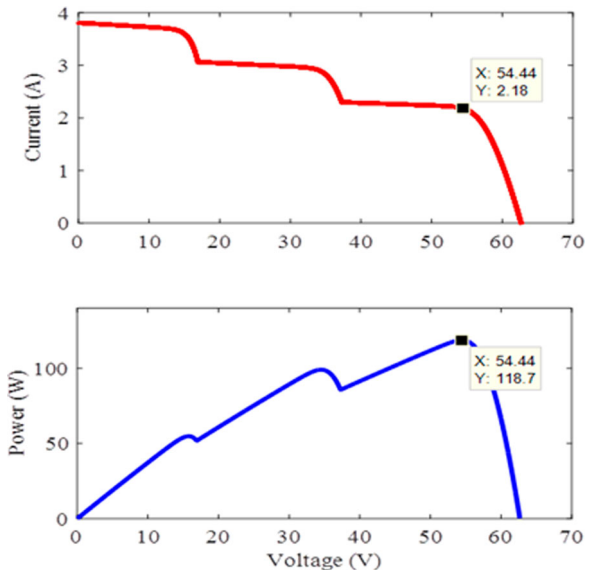

Figure 9. Current-Voltage and Power-Voltage characteristics during PSS-1.

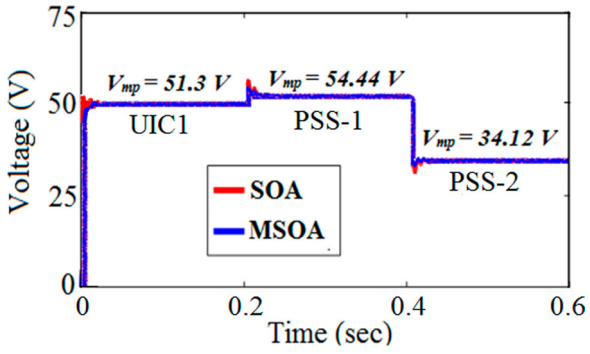

Figure 10. PV voltage during UIC1, PSS-1 and PSS-2.

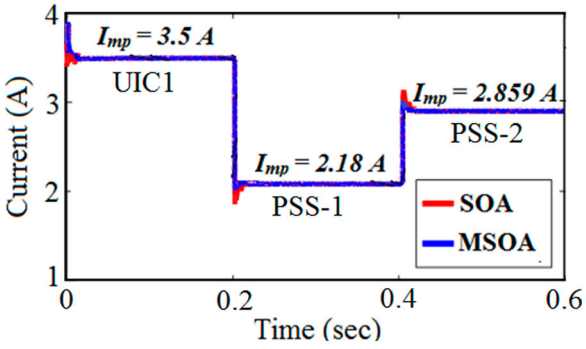

Figure 11. PV current during UIC1, PSS-1 and PSS-2.

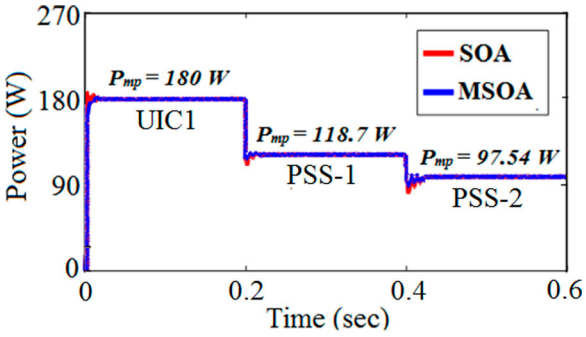

Figure 12. PV power during UIC1, PSS-1 and PSS-2.

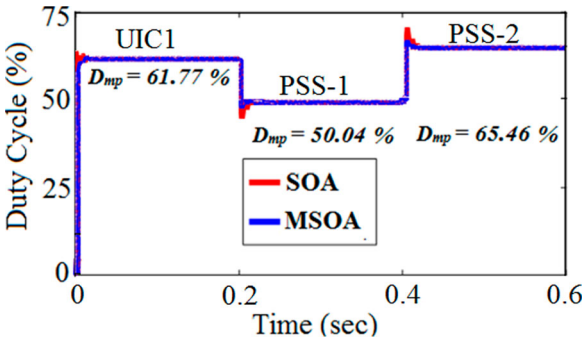

Figure 13. Duty cycle curves during UIC1, PSS-1 and PSS-2.

Table 5. Comparison of SOA and MSOA MPPT approaches under PSS-1.

Parameter	SOA	MSOA	Actual values
PV Power (W)	117.755	117.972	118.7
PV current (A)	2.171	2.173	2.18
PV voltage (V)	54.24	54.29	54.44
Duty cycle (%)	49.84	49.88	50.04
Efficiency (%)	99.20	99.38	100
Settling period (ms)	21.5	20.5	–
Percentage maximum overshoot (%)	3.92	3.02	–

5.3. *Partial Shading Situation 2 (PSS-2)*

During this situation, solar panel 1, solar panel 2 and solar panel 3 gets Sun's insolation of 900, 800 and 400 W/m2, respectively. The solar array's Current-Voltage and Power-Voltage characteristic during PSS-2 is shown in Figure 14. The comparison curves of voltage of PV array, current of PV array and power of PV

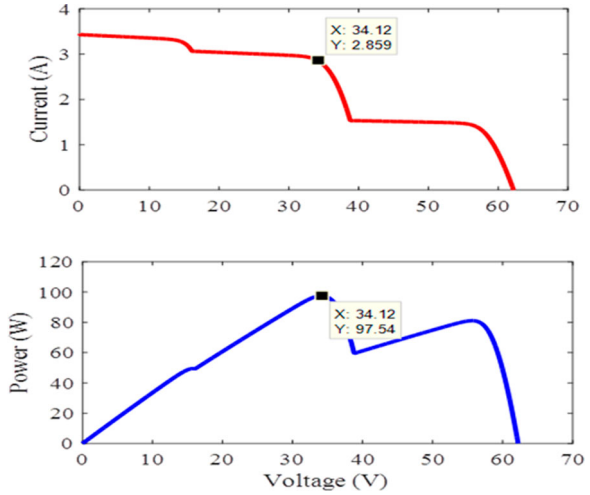

Figure 14. Current-Voltage and Power-Voltage characteristics during PSS-2.

Table 6. Comparison of SOA and MSOA MPPT approaches under PSS-2.

Parameter	SOA	MSOA	Actual values
PV Power (W)	96.491	96.787	97.54
PV current (A)	2.833	2.84	2.859
PV voltage (V)	34.06	34.08	34.12
Duty cycle (%)	65.27	65.32	65.46
Efficiency (%)	98.92	99.22	100
Settling period (ms)	25	23	–
Percentage maximum overshoot (%)	4.15	3.04	–

array for SOA and MSOA MPPT approaches under PSS-2 at 0.4 s are represented in Figure 10–12. The duty cycle curve for MSOA and SOA MPPT approaches is shown in Figure 13 at 0.4 s. Upon the observation from Figure 12, the values of PV power for MSOA and SOA MPPT approaches are 96.787, and 96.491 W, respectively, during PSS-2. The settling times of MSOA and SOA MPPT approaches are 23 and 25 ms, respectively. The MSOA and SOA MPPT approaches' percentage maximum overshoots are 3.04% and 4.15%, respectively. With the results of simulation, it is clearly observed that maximum power is extracted by the suggested MSOA MPPT approach with less time for convergence and less maximum percentage overshoot during PSS-2. The comparison of SOA and MSOA MPPT approaches during PSS-2 is displayed in Table 6.

5.4. Partial Shading Situation 3 (PSS-3)

During this situation, solar panel 1, solar panel 2 and solar panel 3 gets Sun's insolation of 700, 600 and 500 W/m2, respectively. The solar array's Current-Voltage and Power-Voltage characteristic under PSS-3 is shown in Figure 15. The comparison curves of voltage of PV array, current of PV array and power of PV array for SOA and MSOA MPPT approaches under PSS-3 at 0.8 s are represented in Figures 16–18. The duty cycle curve for MSOA and SOA MPPT approaches

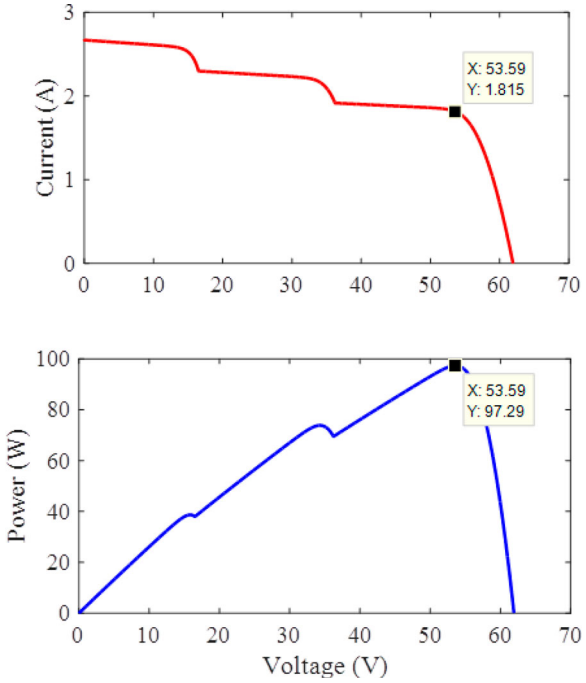

Figure 15. Current-Voltage and Power-Voltage characteristics during PSS-3.

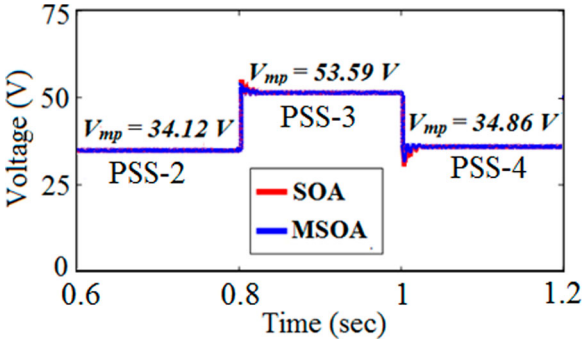

Figure 16. PV voltage during PSS-3 and PSS-4.

is shown in Figure 19 at 0.8 s. Upon observation of the results of simulation in Figure 18 under PSS-3, the values of PV power for MSOA and SOA MPPT approaches are 96.442 and 96.298 W respectively. With MSOA and SOA MPPT approaches, settling times are 26.2 and 32.6 ms, respectively. The MSOA and SOA MPPT approaches' maximum percentage overshoots are 3.07% and 4.33%, respectively. With the results of simulation, it is clearly observed that maximum power is extracted by the suggested MSOA MPPT approach with less time for convergence and less maximum percentage overshoot during PSS-3. The comparison of SOA and MSOA MPPT approaches during PSS-3 is displayed in Table 7.

5.5. Partial Shading Situation 4 (PSS-4)

During this situation, solar panel 1, solar panel 2 and solar panel 3 gets Sun's insolation of 700, 500

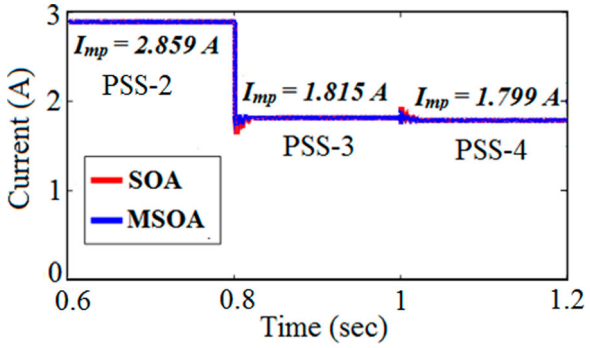

Figure 17. PV current during PSS-3 and PSS-4.

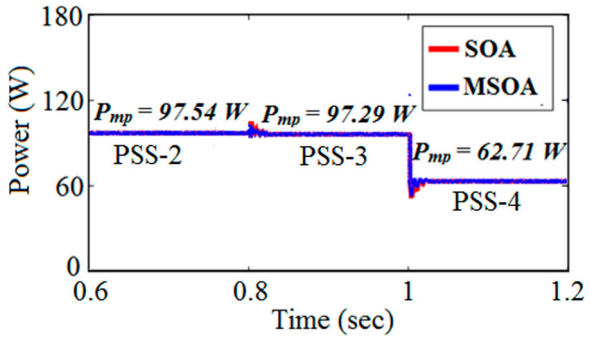

Figure 18. PV power during PSS-3 and PSS-4.

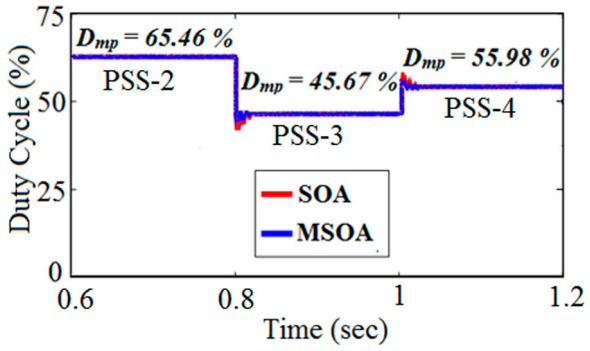

Figure 19. Duty cycle curves during PSS-3 and PSS-4.

Table 7. Comparison of SOA and MSOA MPPT approaches under PSS-3.

Parameter	SOA	MSOA	Actual values
PV Power (W)	96.298	96.442	97.29
PV current (A)	1.802	1.803	1.815
PV voltage (V)	53.44	53.49	53.59
Duty cycle (%)	45.55	45.58	45.67
Efficiency (%)	98.98	99.12	100
Settling period (ms)	32.6	26.2	–
Percentage maximum overshoot (%)	4.33	3.07	–

and 300 W/m2, respectively. The solar array's Current-Voltage and Power-Voltage characteristic during PSS-4 is represented in Figure 20. The comparison curves of voltage of PV array, current of PV array and power of PV array for SOA and MSOA MPPT approaches under PSS-4 are represented at 1 s in Figures 16–18. The duty cycle curve for MSOA and SOA MPPT approaches is shown in Figure 19 at 1 s. Upon observation of

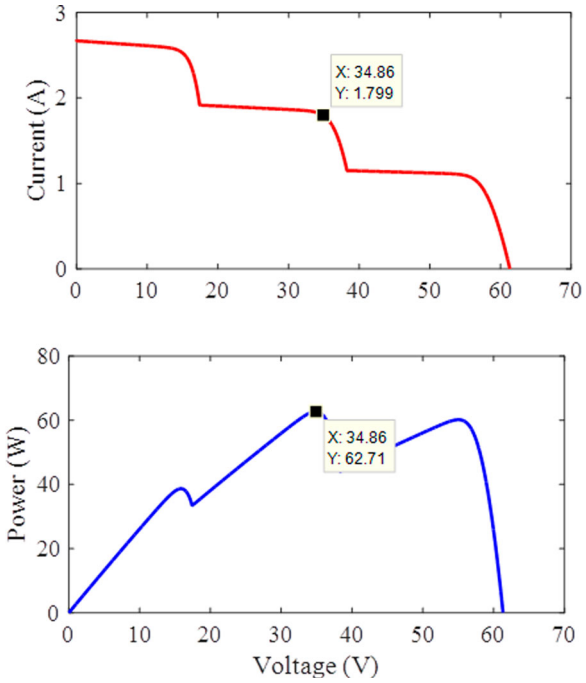

Figure 20. Current-Voltage and Power-Voltage characteristics during PSS-4.

Table 8. Comparison of SOA and MSOA MPPT approaches under PSS-4.

Parameter	SOA	MSOA	Actual values
PV Power (W)	61.976	62.221	62.71
PV current (A)	1.784	1.789	1.799
PV voltage (V)	34.74	34.78	34.86
Duty cycle (%)	55.87	55.91	55.98
Efficiency (%)	98.82	99.22	100
Settling period (ms)	34	28	–
Percentage maximum overshoot (%)	4.55	3.16	–

the results of simulation during PSS-4 in Figure 18, the values of PV power for MSOA and SOA MPPT approaches are 62.221 and 61.976 W, respectively. With MSOA and SOA MPPT approaches, the settling times are 28 and 34 ms, respectively. The MSOA and SOA MPPT approaches' maximum percentage overshoots are 3.16% and 4.55%, respectively. With the results of simulation, it is clearly observed that maximum power is extracted by the suggested MSOA MPPT approach with less time for convergence and less maximum percentage overshoot during PSS-4. The comparison of SOA and MSOA MPPT approaches during PSS-4 is displayed in Table 8.

The comparison of percentage efficiencies, settling times, percentage maximum overshoots of SOA and MSOA MPPT approaches are displayed in Figure 21, Figure 22 and Figure 23, respectively.

The comparison of various MPPT approaches with the proposed MSOA MPPT approach is presented in Table 9. The proposed MSOA MPPT approach is capable of tracking GMPP with very high tracking speed and efficiency with no steady-state oscillations.

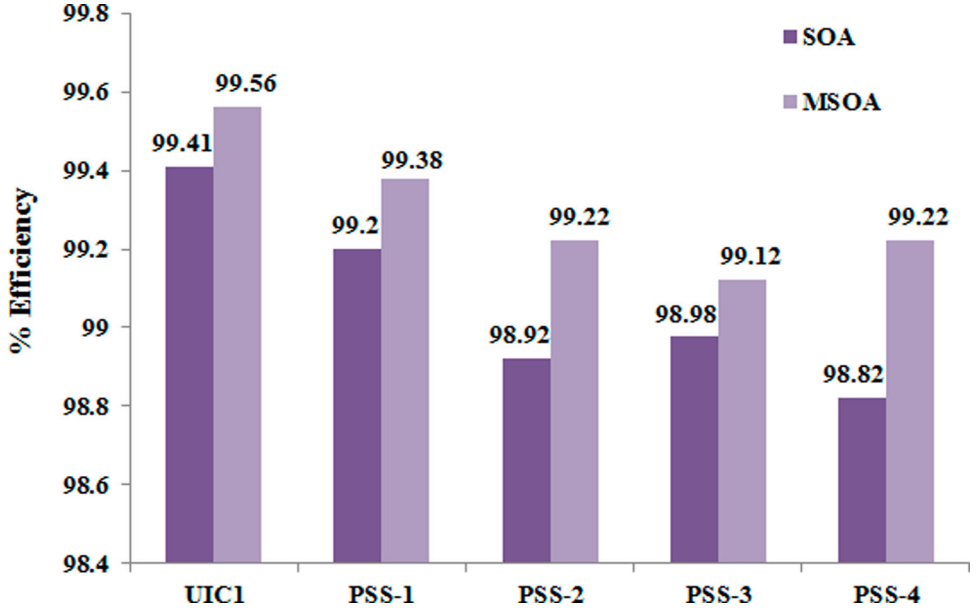

Figure 21. Percentage efficiencies' comparison of SOA and MSOA MPPT approaches.

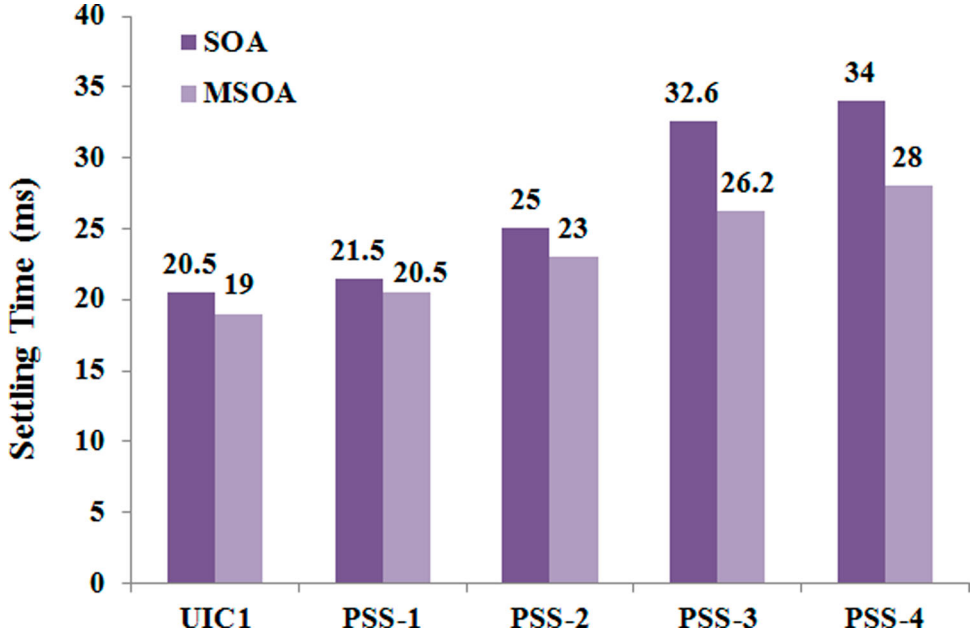

Figure 22. Settling times' comparison of SOA and MSOA MPPT approaches.

Table 9. Comparison of various MPPT approaches with proposed MSOA MPPT approach.

MPPT method	GMPP tracking ability	Tracking speed	Efficiency	Steady state oscillations
P&O, INC [8]	No	High	Low	Yes
PSO [11]	Yes	Medium	High	No
PSO and LFM [30]	Yes	High	High	No
Improved Squirrel Search Algorithm [31]	Yes	High	Very high	No
Jaya Algorith and LFM [32]	Yes	High	Very High	No
Proposed MSOA	Yes	Very high	Very high	No

6. Experimental results

The effectiveness of the MSOA MPPT approach is confirmed with the hardware implementation of the solar PV system. The solar PV system consists of PV array with three series connected PV modules with the rating of each PV module being I_{mp} of 3.5 A, V_{mp} of 17.1 V and P_{mp} of 60 W as mentioned in Table 1. The boost converter with the design values as specified in Table 2 receives its input DC voltage from the PV array. At the boost converter's output, a DC load of 120 ohms resistance is connected. The microcontroller dsPIC30F4011 receives the PV array's current and voltage values from the current and voltage sensors respectively and produces the Pulse Width Modulation signal for the boost converter's MOSFET switch in accordance to the MSOA MPPT approach thereby fixing optimal boost converter's duty cycle that corresponds to GMPP. The hardware implementation setup of MSOA MPPT approach is shown in Figure 24. The results of hardware implementation during UIC1, PSS-1 and PSS-2, PSS-3

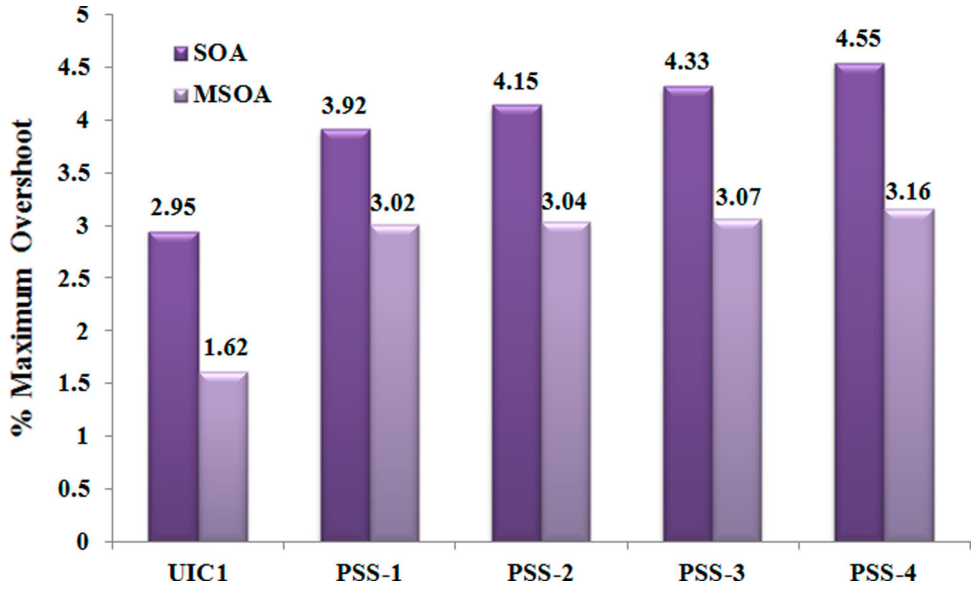

Figure 23. Maximum percentage overshoots' comparison of SOA and MSOA MPPT approaches.

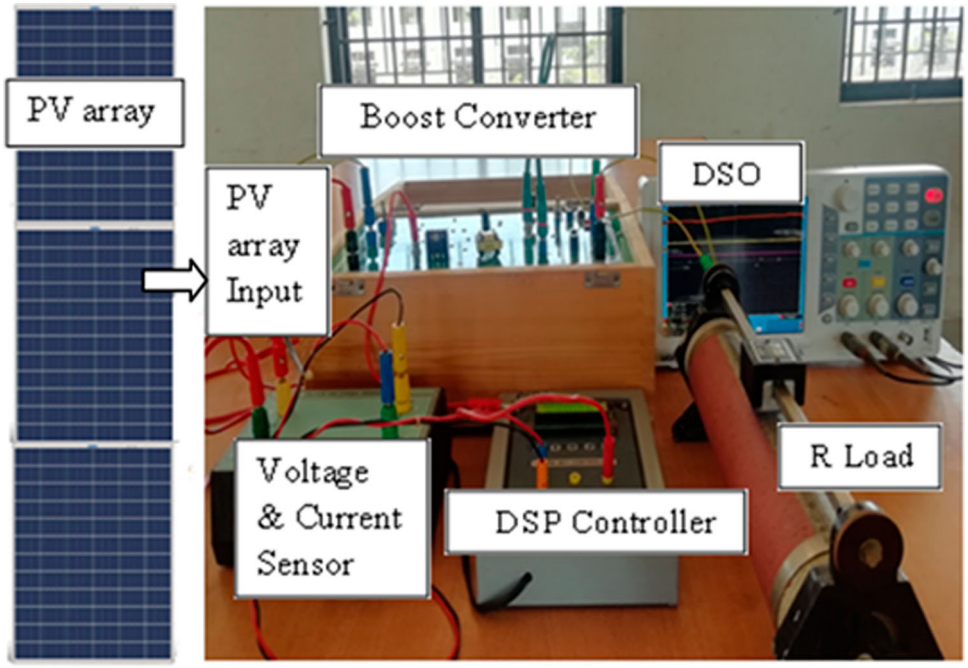

Figure 24. Hardware implementation of MSOA MPPT approach.

and PSS-4 are shown in Figure 25, Figure 26 and Figure 27 respectively.

With the implementation of experimental setup, it is noted that under UIC1, PSS-1, PSS-2, PSS-3 and PSS-4, the values of PV power are 179.20, 117.95, 96.76, 96.42 and 62.20 W with settling periods of 20, 21, 25, 28 and 28.5 ms, respectively. The experimental results agree well with the results of simulation in quick achieving of GMPP authenticating the proposed MPPT approach based on MSOA for solar PV systems.

7. Conclusion

This paper suggested a Modified Seagull Optimization Algorithm (MSOA) MPPT, that is proficient and has the capability to determine the solar array's GMPP during uniform irradiation situations and partial shading situations. The Levy Flight Mechanism (LFM) incorporated into the original SOA aided in a better compromise between the exploration capability and exploitation capability of SOA due to the randomness nature introduced by LFM, and the jump size determined by Levy probability distribution function augmented the exploration capability that helped in avoidance of the local maxima trapping. The incorporation of the formula for heat exchange of TEO in SOA ensured the modification of duty cycle values in a slower pace near the target duty cycle, which ensured good accuracy. The results of simulation validated the accuracy in tracking of GMPP by MSOA MPPT method with higher efficiency, less maximum percentage overshoot and less time of convergence in comparison to SOA MPPT

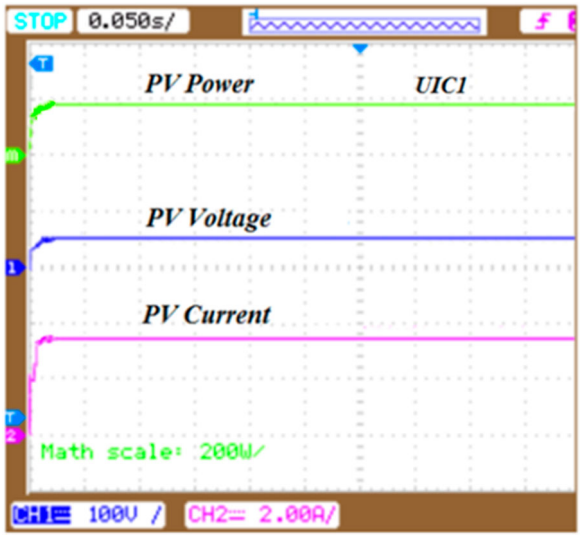

Figure 25. Results of experimentation for MSOA MPPT under UIC1.

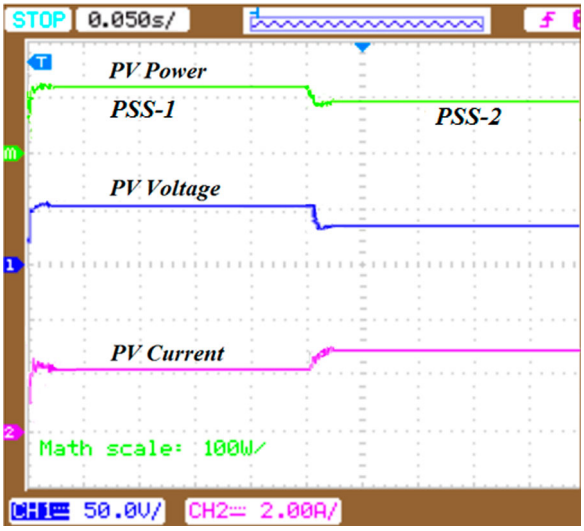

Figure 26. Results of experimentation for MSOA MPPT under PSS-1 and PSS-2.

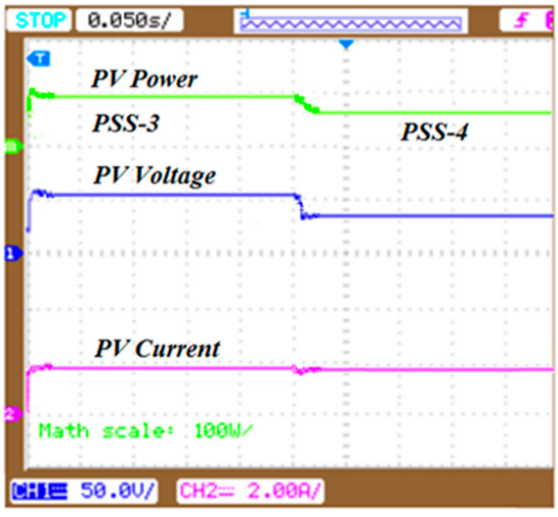

Figure 27. Results of experimentation for MSOA MPPT under PSS-3 and PSS-4.

method during uniform irradiation situation and partial shading situations, which are also confirmed with the results of hardware implementation. The MSOA MPPT can be applied to any single switch DC-DC boost converters with multiple peaks in the P-V curve and its performance analysis can be considered as future work.

Disclosure statement

No potential conflict of interest was reported by the author(s).

References

[1] Paz F, Ordonez M. High-performance solar MPPT using switching ripple identification based on a lock-in amplifier. IEEE Trans Ind Electron. 2016;63(6):3595–3604. DOI: 10.1109/TIE.2016.2530785.

[2] Chikh A, Chandra A. An optimal maximum Power Point Tracking Algorithm for PV systems with climatic parameters estimation. IEEE Trans Sustainable Energy. 2015;6(2):644–652. DOI: 10.1109/TSTE.2015.2403845.

[3] Metry M, Shadmand MB, Balog RS, et al. MPPT of Photovoltaic systems using sensorless current-based model predictive control. IEEE Trans Ind Appl. 2017;53(2):1157–1167. DOI: 10.1109/TIA.2016.2623283.

[4] Kumar N, Hussain I, Singh B, et al. Normal harmonic search algorithm-based MPPT for solar PV system and integrated with grid using reduced sensor approach and PNKLMS algorithm. IEEE Trans Ind Appl. 2018;54(6):6343–6352. DOI: 10.1109/TIA.2018.2853744.

[5] Adhikari S, Li F. Coordinated V-f and P-Q control of solar Photovoltaic generators with MPPT and battery storage in microgrids. IEEE Trans Smart Grid. 2014;5(3):1270–1281. DOI: 10.1109/TSG.2014.2301157.

[6] Diab-Marzouk A, Trescases O. SiC-Based bidirectional Ćuk converter with differential power processing and MPPT for a solar powered aircraft. IEEE Trans Transp Electrification. 2015;1(4):369–381. DOI: 10.1109/TTE.2015.2505302.

[7] Tan CY, Rahim NA, Selvaraj J. Improvement of hill climbing method by introducing simple irradiance detection method, 3rd IET International Conference on Clean Energy and Technology (CEAT) 2014, Kuching, 2014, p. 1–5, DOI: 10.1049/cp.2014.1493.

[8] Sera D, Mathe L, Kerekes T, et al. On the perturb-and-observe and incremental conductance MPPT methods for PV systems. IEEE Journal of Photovoltaics. 2013;3(3):1070–1078. DOI: 10.1109/JPHOTOV.2013.2261118.

[9] Naveen and Dahiya AK, Implementation and comparison of perturb & observe, ANN and ANFIS based MPPT techniques, 2018 International Conference on Inventive Research in Computing Applications (ICIRCA), Coimbatore, 2018, p. 1–5, DOI: 10.1109/ICIRCA.2018.8597271.

[10] Raghuwanshi SS and Khare V., FLC based MPPT controller for optimal tracking photovoltaic system, 2017 International Conference on Information, Communication, Instrumentation and Control (ICICIC), Indore, 2017, p. 1–6, DOI: 10.1109/ICOMICON.2017.8279018.

[11] Abdullah MA, Al-Hadhrami T, Tan CW, et al. Towards Green energy for Smart cities: particle swarm optimization based MPPT approach. IEEE Access.

2018;6:58427–58438. DOI: 10.1109/ACCESS.2018.2874525.

[12] Eltamaly AM, Al-Saud MS, Abokhalil AG. A Novel Bat Algorithm strategy for maximum power point tracker of Photovoltaic energy systems under dynamic partial shading. IEEE Access. 2020;8:10048–10060. DOI: 10.1109/ACCESS.2020.2964759.

[13] Sundareswaran K, Sankar P, Nayak PSR, et al. Enhanced energy output from a PV system under partial shaded conditions through Artificial Bee Colony. *IEEE Trans Sustain Energy*. 2015;6(1):198–209. DOI: 10.1109/TSTE.2014.2363521.

[14] Mohammad L, Prasetyono E, Murdianto FD. Performance evaluation of ACO-MPPT and constant voltage method for street lighting charging system, 2019 International Seminar on Application for Technology of Information and Communication (iSemantic), Semarang, Indonesia, 2019, p. 411–416, DOI: 10.1109/ISEMANTIC.2019.8884303.

[15] Nugraha DA, Lian KL, Suwarno. A novel MPPT method based on Cuckoo Search Algorithm and Golden Section Search Algorithm for partially shaded PV system. Can J Electr Comput Eng. 2019;42(3):173–182. DOI: 10.1109/CJECE.2019.2914723.

[16] Prasanth Ram J, Rajasekar N. A Novel Flower Pollination based Global Maximum Power Point method for Solar Maximum Power Point Tracking. IEEE Trans Power Electron. 2017;32(11):8486–8499. DOI: 10.1109/TPEL.2016.2645449.

[17] Kumar C, Rao R. A novel global MPP tracking of a Photovoltaic system based on Whale Optimization Algorithm. Int J Renew Energy Dev. 2016;5(3):225–232.

[18] Mohanty S, Subudhi B, Ray PK. A new MPPT design using grey wolf optimization technique for Photovoltaic system under partial shading conditions. IEEE Trans Sustainable Energy. 2016;7(1):181–188.

[19] Yang B, Zhong L, Zhang X, et al. Novel bio-inspired memetic Salp Swarm algorithm and application to MPPT for PV systems considering partial shading condition. J Clean Prod. 2019;215:1203–1222.

[20] Yousri D, Babu TS, Beshr E, et al. A robust strategy based on marine predators algorithm for large scale photovoltaic array reconfiguration to mitigate the partial shading effect on the performance of PV system. IEEE Access. 2020;8:112407–112426.

[21] Ibrahim A-w, et al. PV maximum power-point tracking using modified particle swarm optimization under partial shading conditions. Chin J Electr Eng. 2020;6(4):106–121. DOI: 10.23919/CJEE.2020.000035.

[22] Guo K, Cui L, Mao M, et al. An improved Gray Wolf Optimizer MPPT Algorithm for PV system with BFBIC converter under partial shading. IEEE Access. 2020;8:103476–103490. DOI: 10.1109/ACCESS.2020.2999311.

[23] Wolpert DH, Macready WG. No free lunch theorems for optimization. IEEE Trans Evol Comput. 1997;1(1):67–82.

[24] Singh P, Dhiman G, Kaur A. A quantum approach for time series data based on graph and Schrodinger equations methods. Mod Phys Lett A. In press, 2018;33:1850208-1–1850208-23. DOI: 10.1142/S0217732318502085.

[25] Dhiman G, Kumar V. Seagull optimization algorithm: theory and its applications for large-scale industrial engineering problems. Knowl Based Syst. 2019;165:169–196. DOI: 10.1016/j.knosys.2018.11.024.

[26] Cao Y, Li Y, Zhang G, et al. Experimental modeling of PEM fuel cells using a new improved Seagull Optimization Algorithm. Energy Rep. 2019;5:1616–1625. DOI: 10.1016/j.egyr.2019.11.013.

[27] Lei G, Song H, Rodriguez D. Power generation cost minimization of the grid-connected hybrid renewable energy system through optimal sizing using the modified Seagull Optimization technique. Energy Rep. 2020;6:3365–3376. DOI: 10.1016/j.egyr.2020.11.249.

[28] Jia H, Xing Z, Song W. A new hybrid Seagull Optimization Algorithm for feature selection. IEEE Access. 2019;7:49614–49631. DOI: 10.1109/ACCESS.2019.2909945.

[29] Liu Y, Cao B. A Novel Ant Colony Optimization Algorithm with Levy Flight. IEEE Access. 2020;8:67205–67213. DOI: 10.1109/ACCESS.2020.2985498.

[30] Chanuri Charin, Dahaman Ishak, Muhammad Ammirrul Atiqi Mohd Zainuri, Baharuddin Ismail, Mohamad Kamarol Mohd Jamil, A hybrid of bio-inspired algorithm based on Levy flight and particle swarm optimizations for photovoltaic system under partial shading conditions, Sol Energy, vol. 217, pp. 1-14, 2021, DOI: 10.1016/j.solener.2021.01.049

[31] Fares D, Fathi M, Shams I, et al. A novel global MPPT technique based on squirrel search algorithm for PV module under partial shading conditions. Energy Convers Manage. 2021;230; DOI: 10.1016/j.enconman.2020.113773.

[32] Motamarri R, Bhookya N. JAYA Algorithm based on Lévy Flight for Global MPPT under partial shading in Photovoltaic system. IEEE J Emerg Sel Top Power Electron. 2021;9(4):4979–4991. DOI: 10.1109/JESTPE.2020.3036405.